Université de Montréal

Cyclic thermal signature in a global MHD simulation of solar convection

Jean-François Cossette
(Université de Montréal)

Paul Charbonneau
(Université de Montréal)

Piotr Smolarkiewicz
(European Center for Medium-Range Weather Forecasts)

NSERC CRSNG

2014 SORCE Science Meeting,
Cocoa Beach, Florida

ECMWF

OUTLINE

- What are the causes of both short-term and long-term TSI variations? : Two schools of thought

#1: All TSI variations are to be attributed to changes in the surface coverage by magnetic structures (i.e. sunspots, faculae & network)

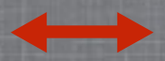

#2 : Pure surface effects alone cannot account for decadal & longer variations: Another type of mechanism is needed, such as a global modulation of the solar thermodynamic structure.

- Observational evidence for global structural changes
- Results from Global MHD simulations of solar convection
- Inferring observational evidence for structural changes from MHD simulations
- Summary & Conclusions

Total solar irradiance variations

Total solar irradiance is the total electromagnetic power per meter-square received at a distance of 1AU from the Sun.

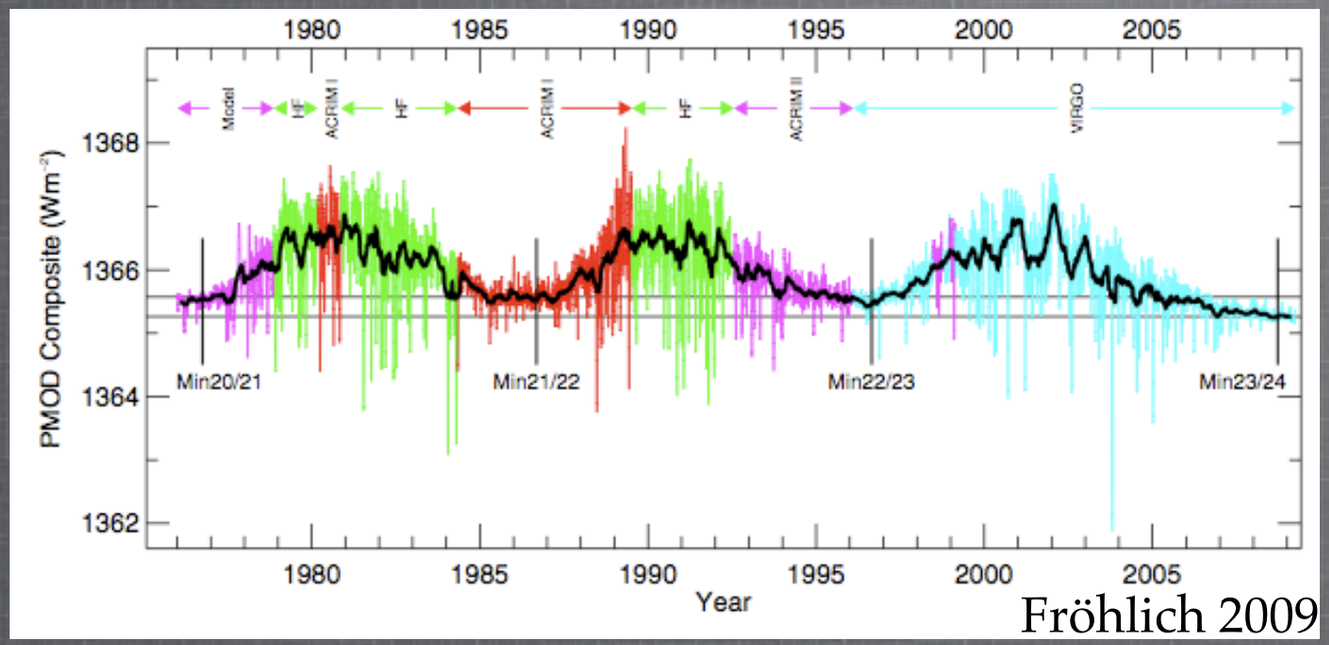

Fröhlich 2009

TSI varies on time scales from minutes to days and months, as well as on the longer time scale of the 11-year solar cycle (e.g. Fröhlich & Lean 2004).

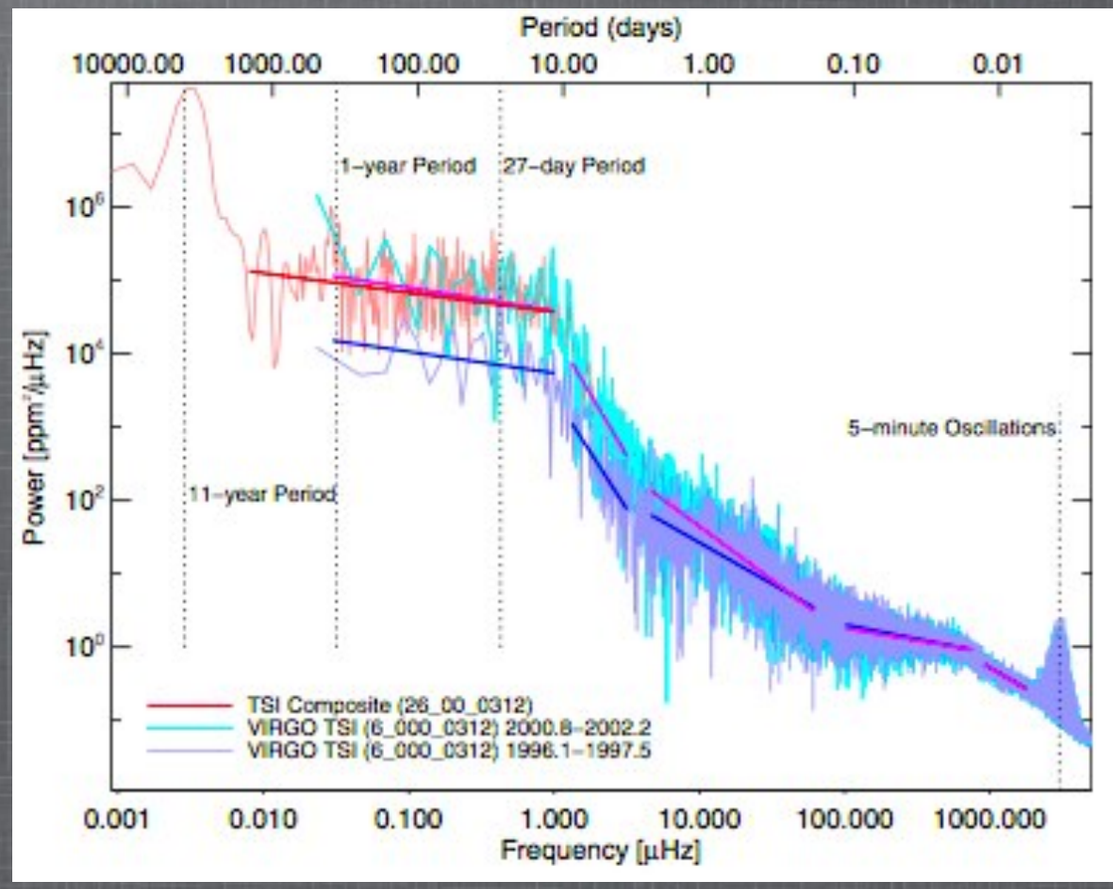

"Short-term" variations (less than a decade)

-Sunspots & faculae (rotational period)

-p-modes (5 min.)

-Large flares (seconds)

"Long-term" variations (decadal and longer)

-11 year solar cycle

-Grand Minima (e.g. Maunder, Dalton, Wolf, Oort)

-Gleissberg (90 yrs.), de Vries (207 yrs.), Eddy(950 yrs.) and Hallstatt (2200 years) [Abreu et al. 2010]

Physical causes of TSI variations

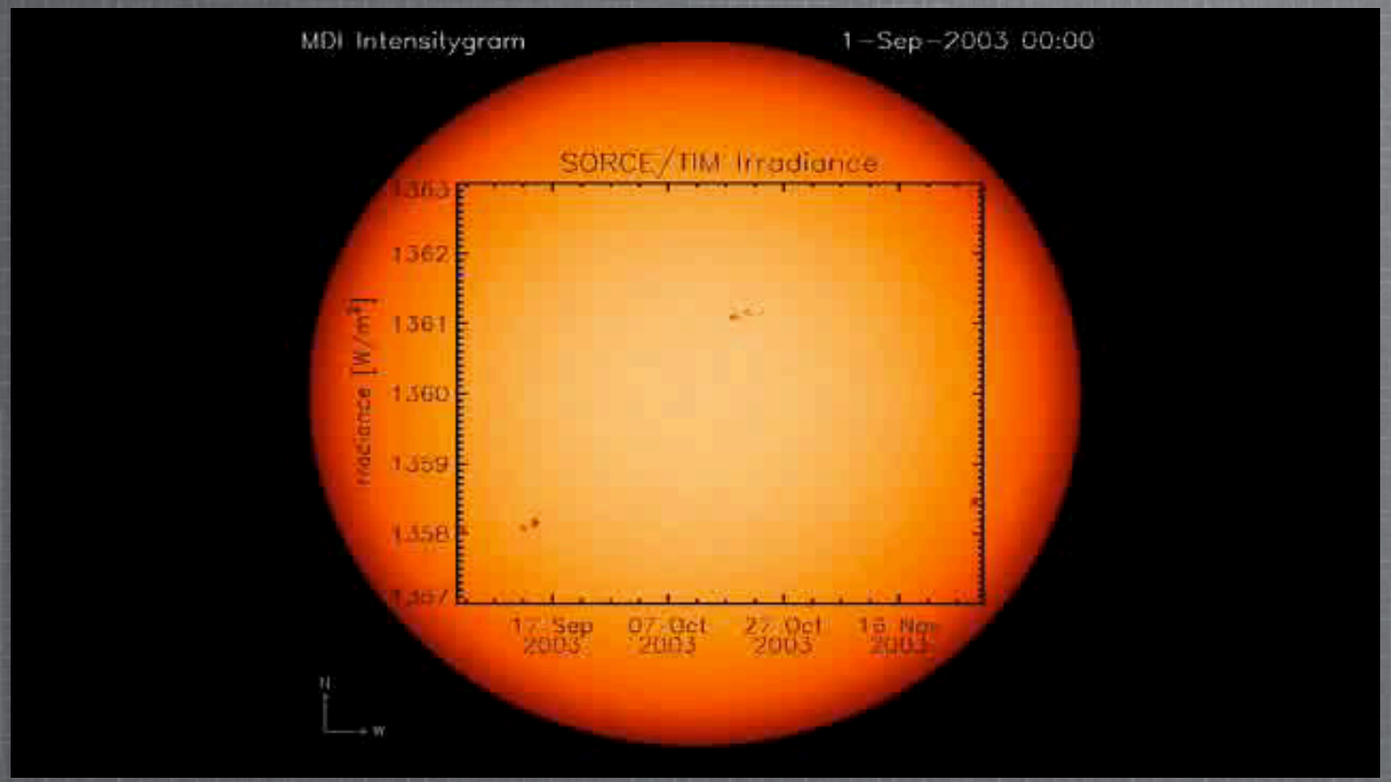

Credit: NASA/Goddard SFC/Glory

http://solarscience.msfc.nasa.gov/images/faculae.jpg

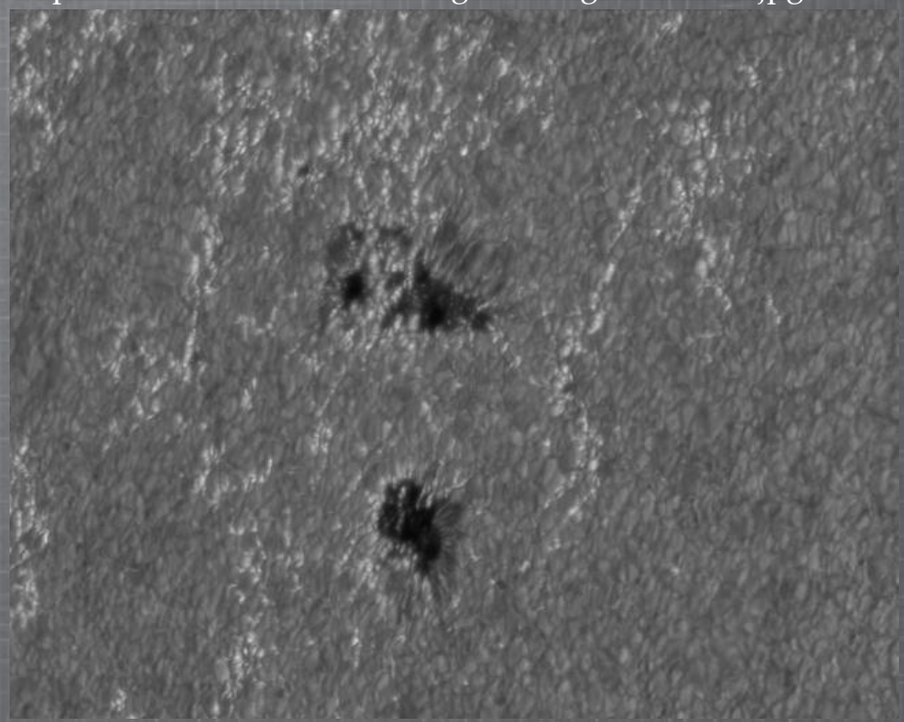

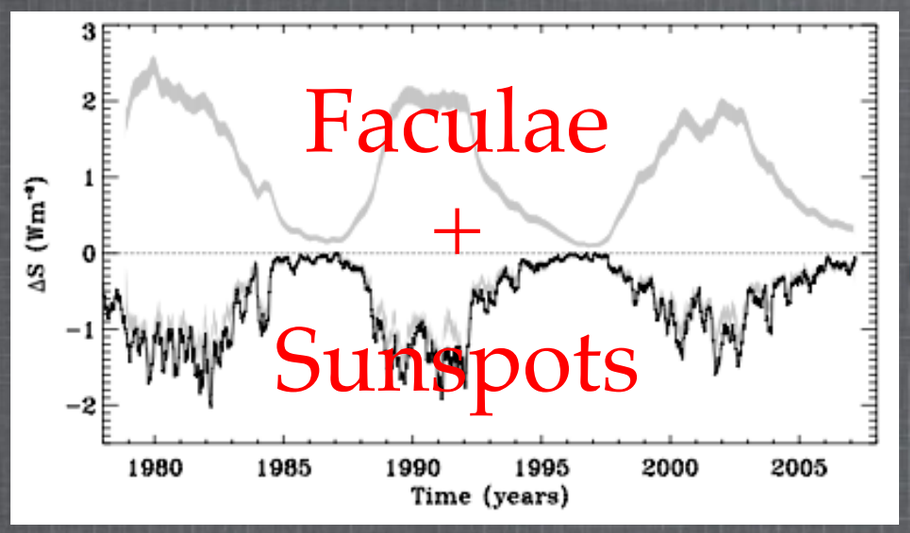

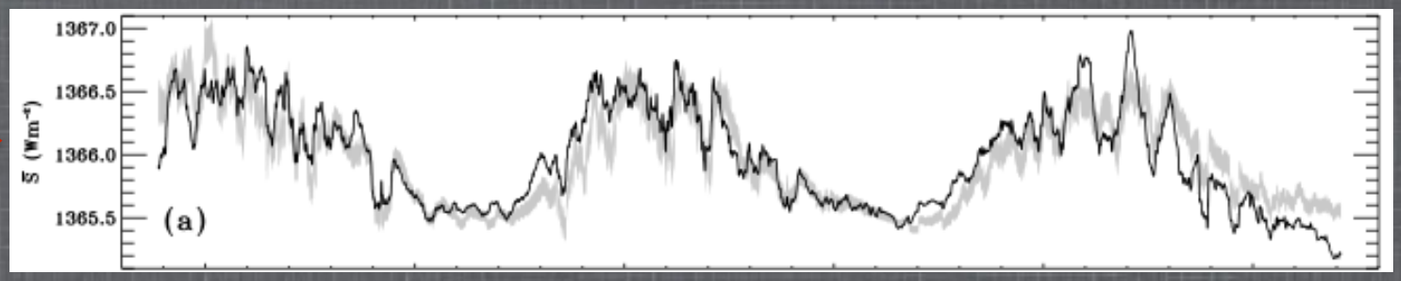

Reconstructed irradiance time series (Crouch et al. 2008)

1st school of thought: The entire TSI variance (i.e. both short-term and long-term variations) is the result of changes ***at the surface*** due to sunspots, faculae and other magnetic structures *(e.g. Foukal & Lean 1996, Chapman 1996, Lean et al. 1996).*

TSI Reconstructions based on pure surface effects

Models that assume only the contribution from sunspots and faculae reproduce the short term variations to an amazing level of accuracy.

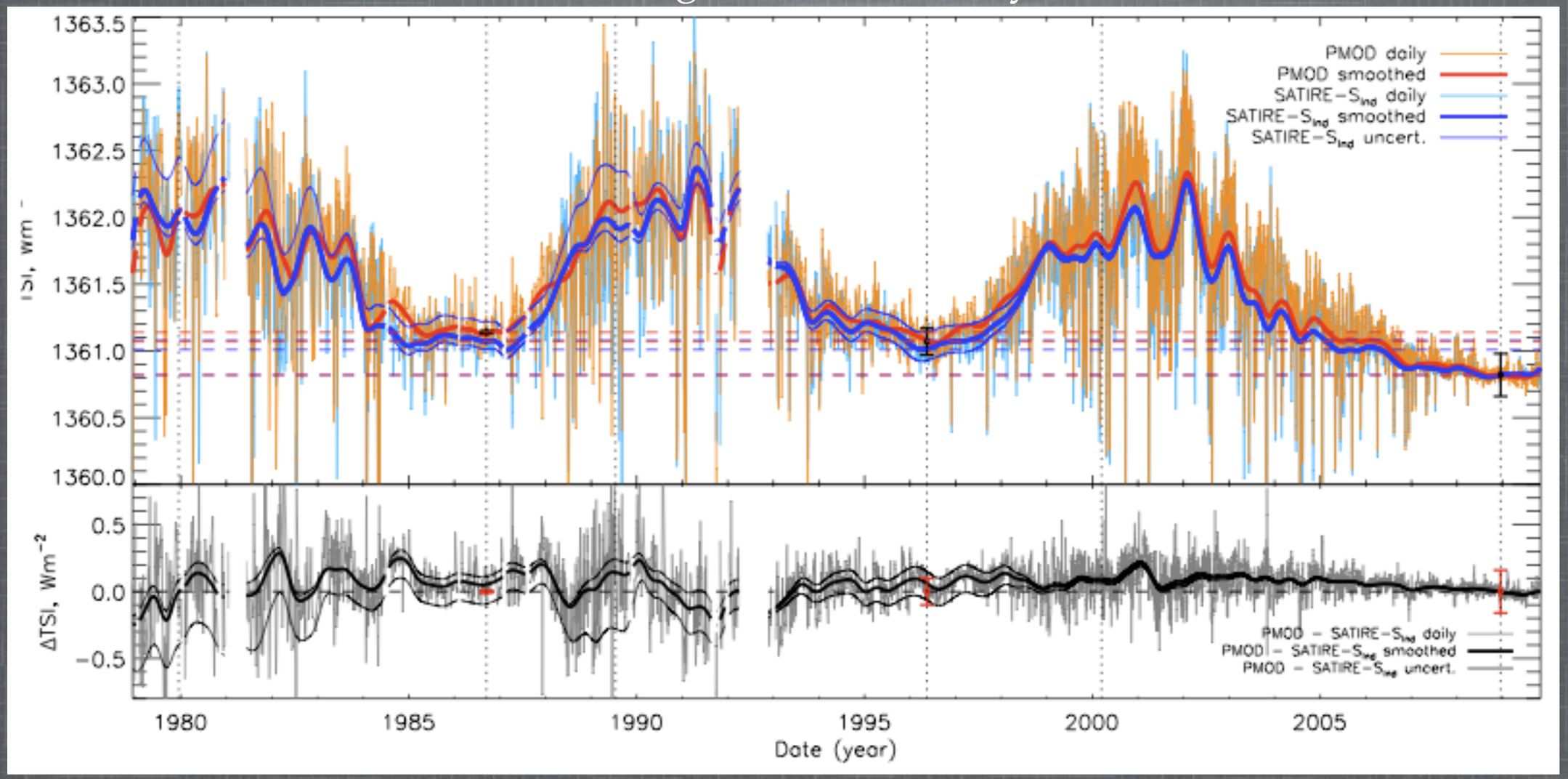

Models can explain up to ~92% of the PMOD composite TSI variance (Ball W.T. et al. 2012).

2nd school of thought: surface magnetism does not explain both short and long term variations; global structural changes need to be taken into account to reproduce the full TSI variance *(Kuhn 1988, Li et al. 2003, Fröhlich 2009, Gray & Livingston 1997).*

Structural changes & Observational Data (1)

(1) A positive correlation between magnetic activity indices and p-mode frequency shifts (Woodward 1987)

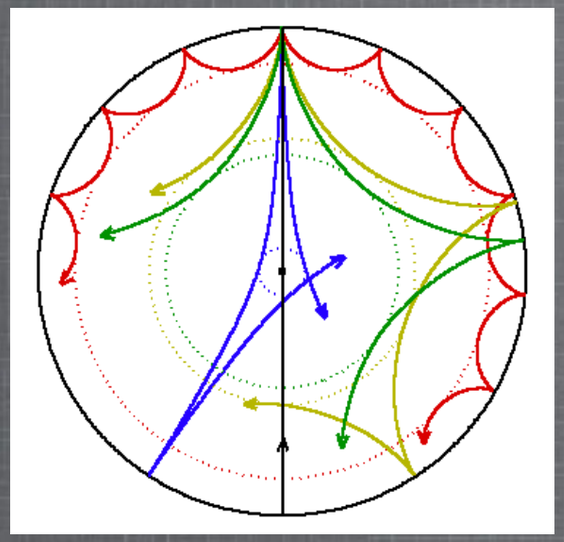

http://soi.stanford.edu/press/ssu8-97/rivers/rays2.gif

$$\delta\nu(t) = \sum_{nl} \frac{Q_{nl}}{\sigma_{nl}^2}\, \delta\nu_{nl}(t) / \sum_{nl} \frac{Q_{nl}}{\sigma_{nl}^2},$$

(Bhatnagar et al.1999)

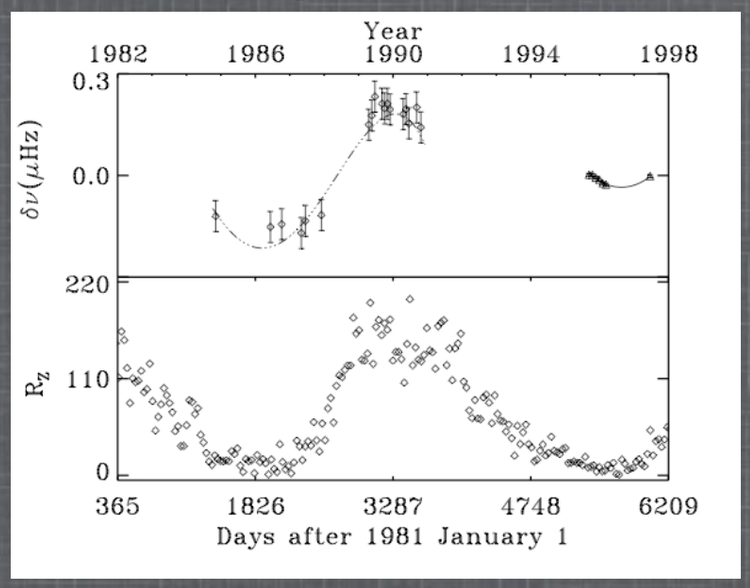

FITTING AND CORRELATION STATISTICS FOR $2 \leq l \leq 150$

Activity Index	Slope a	Intercept b (μHz)	χ^2	r_P	P_P	r_S	P_S
R_I	0.002 ± 0.0001 μHz	-0.034 ± 0.001	344	0.82	0.023	0.93	0.002
KPMI	0.029 ± 0.001 μHz G^{-1}	-0.221 ± 0.008	461	0.81	0.025	0.71	0.071
F_{10}	0.005 ± 0.0002 μHz sfu^{-1}	-0.345 ± 0.011	144	0.93	0.002	0.93	0.002
He I	0.010 ± 0.0004 μHz mÅ^{-1}	-0.449 ± 0.017	480	0.76	0.049	0.61	0.148
SMMF	0.0004 ± 0.0002 μHz μT^{-1}	-0.009 ± 0.002	1130	0.16	0.729	0.21	0.645
MPSI	0.191 ± 0.006 μHz G^{-1}	-0.031 ± 0.0009	266	0.87	0.011	0.93	0.002
FI	0.023 ± 0.0008 μHz	-0.017 ± 0.0005	373	0.83	0.020	0.93	0.002
Fe XIV	0.012 ± 0.0004[a]	-0.048 ± 0.001	128	0.93	0.006	0.94	0.005
Mg II	38.210 ± 1.172 μHz	-9.712 ± 0.297	68	0.97	0.003	0.90	0.005

[a] In units of μHz sr/10^{16} W.

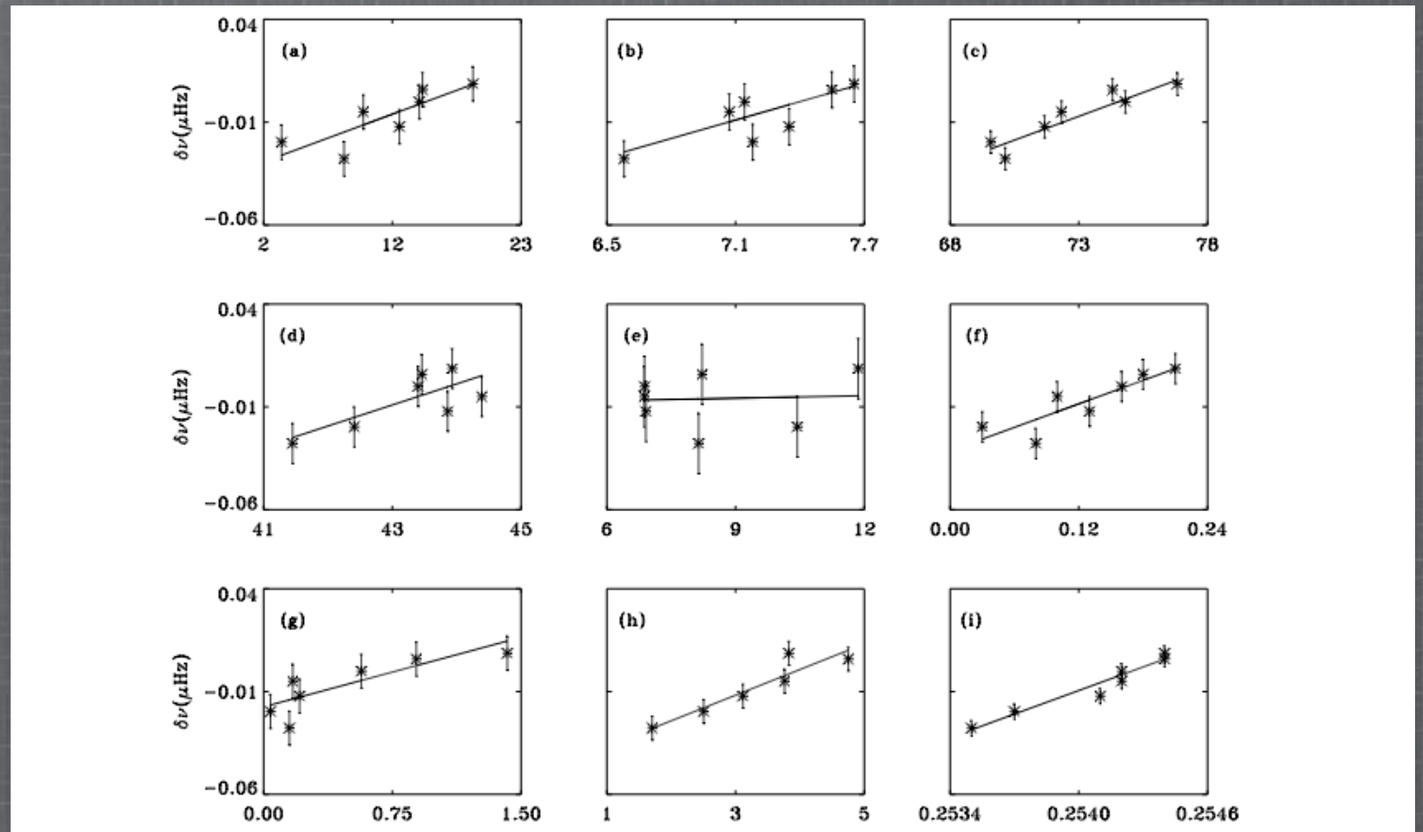

FIG. 2.—Comparison of weighted mean frequency shift with nine different activity indices in the l-range of 2–150. These are (*a*) the sunspot number, (*b*) the Kitt Peak magnetic index (G), (*c*) the 10.7 cm flux (sfu), (*d*) the He I λ10830 equivalent width (mÅ), (*e*) the Stanford mean magnetic field (μT), (*f*) the magnetic plage strength index (G), (*g*) the total flare index, (*h*) the coronal line intensity (10^{16} W sr^{-1}), and (*i*) the Mg II core-to-wing ratio. The solid line represents the linear fit. The error bars indicate 1 σ error of the fitting.

Structural changes & Observational Data (1)

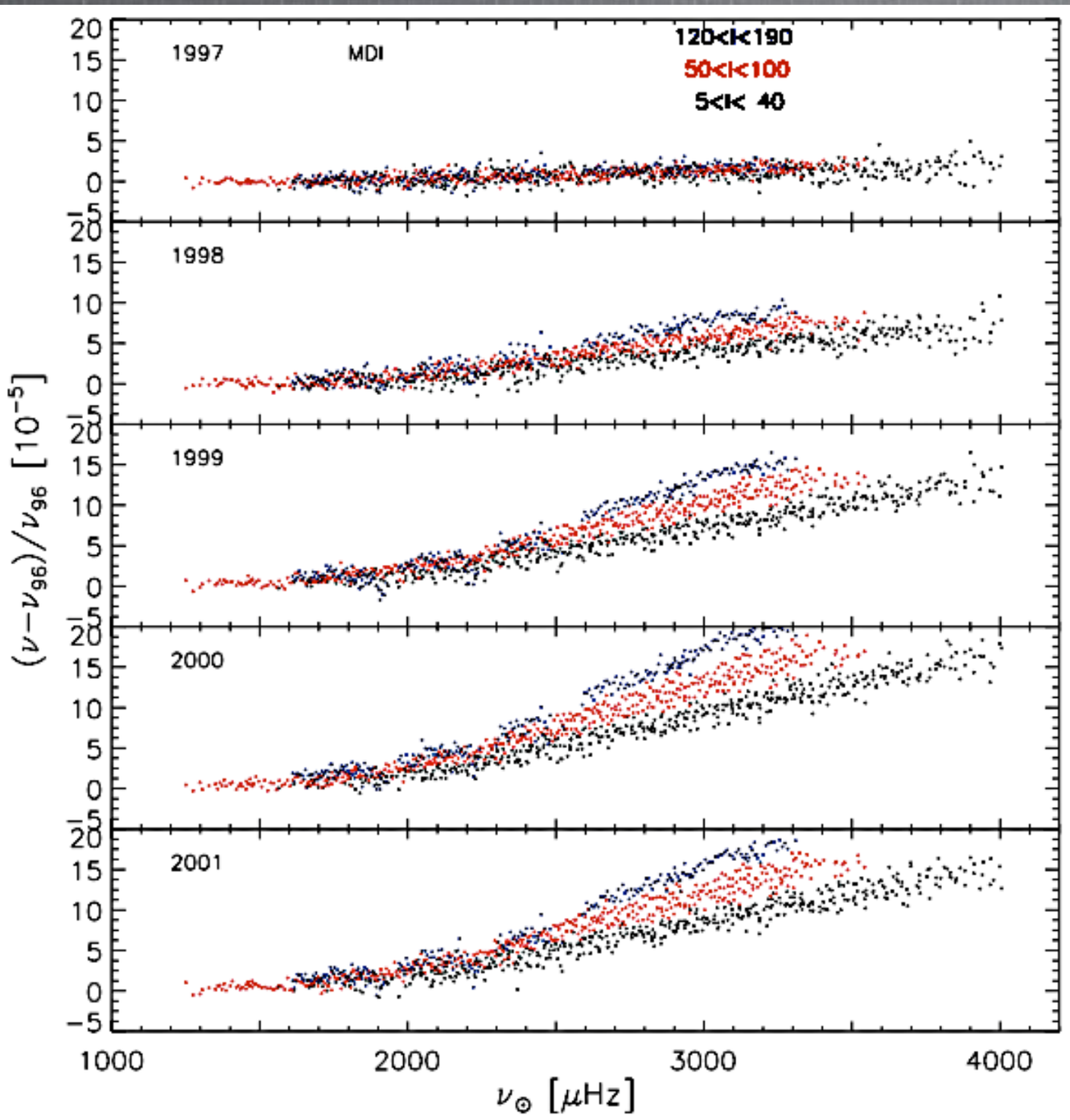

FIG. 1.—Observed relative *p*-mode frequency variations by MDI as functions of frequency and angular degree

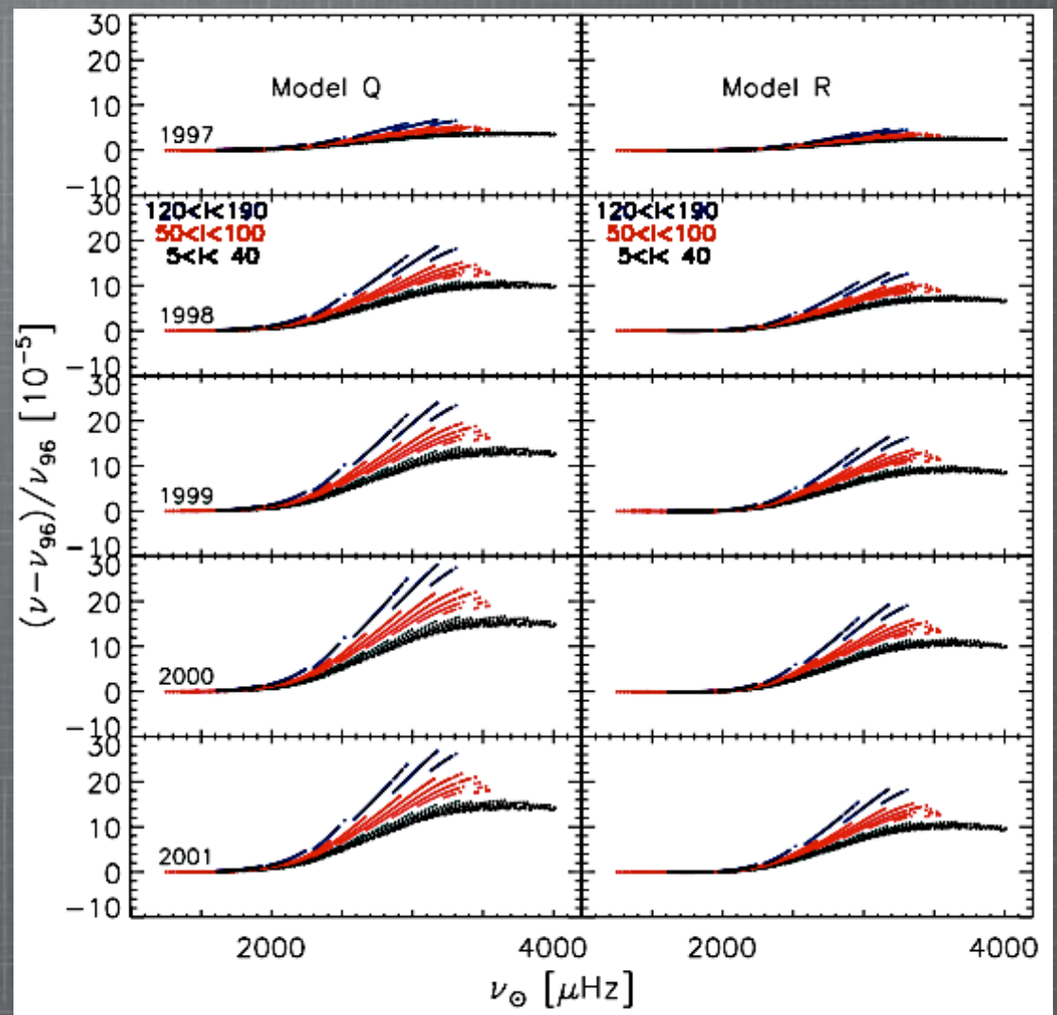

FIG. 15.—Calculated relative frequency variations for models Q–R as functions of frequency

1D structural model including a magnetically-modulated turbulent mechanism (Li et al 2003).

Obtaining a complete physical picture of a potential global modulating mechanism requires the use of self-consistent physical models.

Structural changes & Observational Data (2)

(2) A long-term trend in TSI, which is not observed in other indicators of magnetic activity.

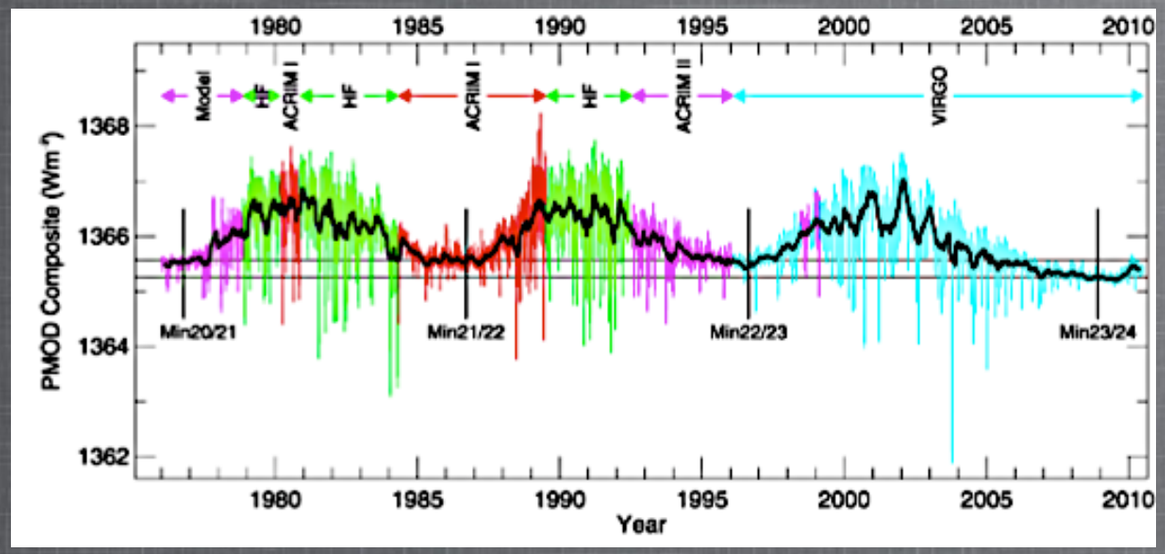

Change of minima over each cycle in percent

TSI	–	6.0	−12.9	**−25.0**	−10.6	15.6	−15.5
B_R	–	5.0	−17.4	**−45.8**	−19.4	25.5	−25.4
SSN	0.8	1.0	−4.7	−4.3	−2.7	3.2	−2.7
F10.7	0.8	−1.6	0.1	−4.0	−1.8	2.1	−1.2
Ly-α	–	4.3	−7.3	−3.4	−2.1	5.9	−3.9
CaII K	–	−1.6	−2.7	−1.5	−1.9	0.7	0.1
MgII	–	0.3	1.8	−2.8	−0.2	2.3	−1.6

(Fröhlich et al. 2013, Fröhlich 2009.)

(3) Long-term SSI trends observed by SORCE consistent with a shallower photospheric temperature gradient (Fontenla et al. 2006, 2007). The later could be due to a reduction of the Rosseland mean opacity, or to an increased energy flow via the magnetic field or by convective motions (Harder et. al 2009).

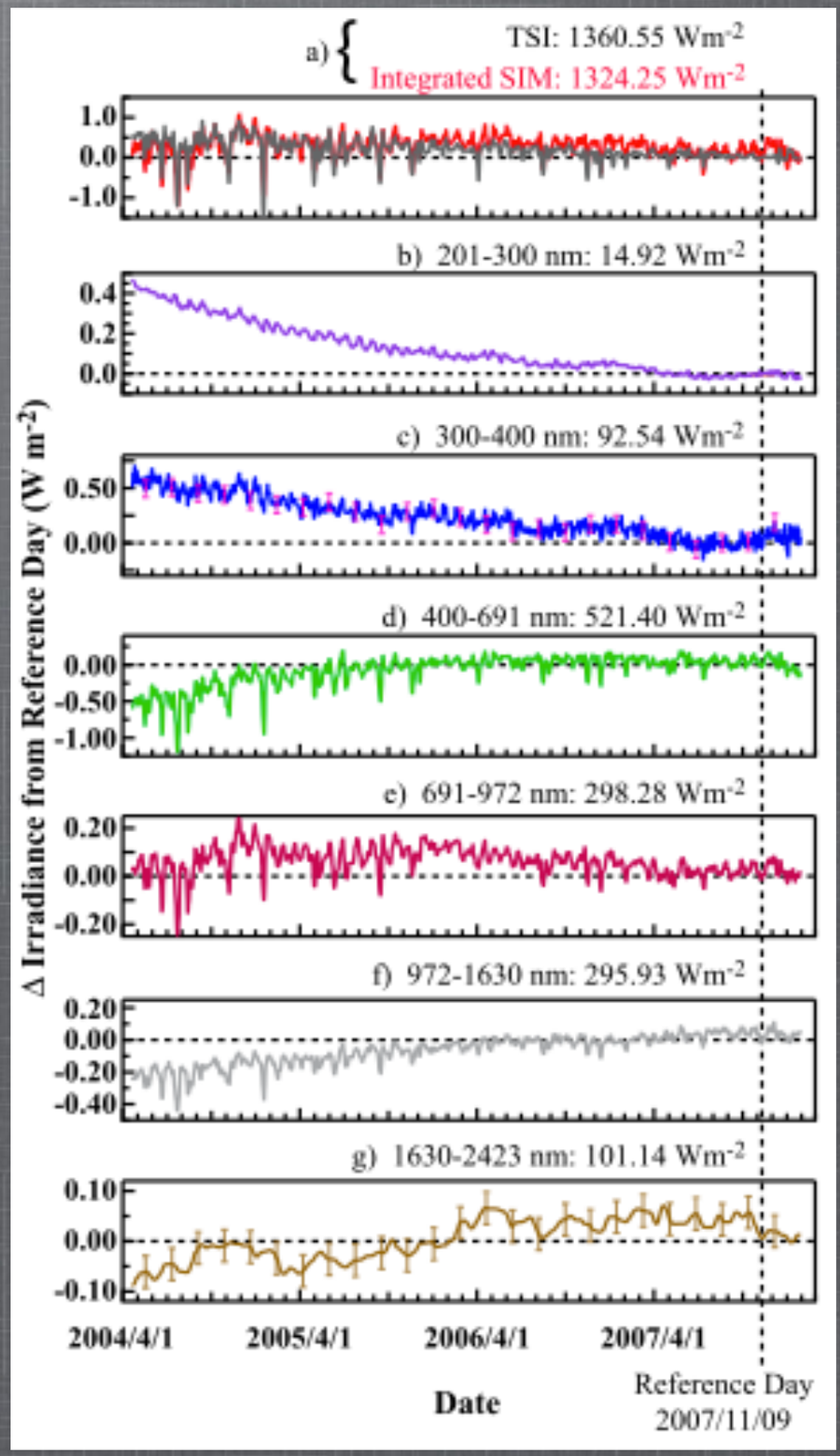

Structural changes & Observational Data (3)

-Surface temperature changes (Gray & Livingtson 1987, Kuhn et al. 1988)

Criticism: Is the temperature excess really originating from the photospheric continuum, and not from faculae?

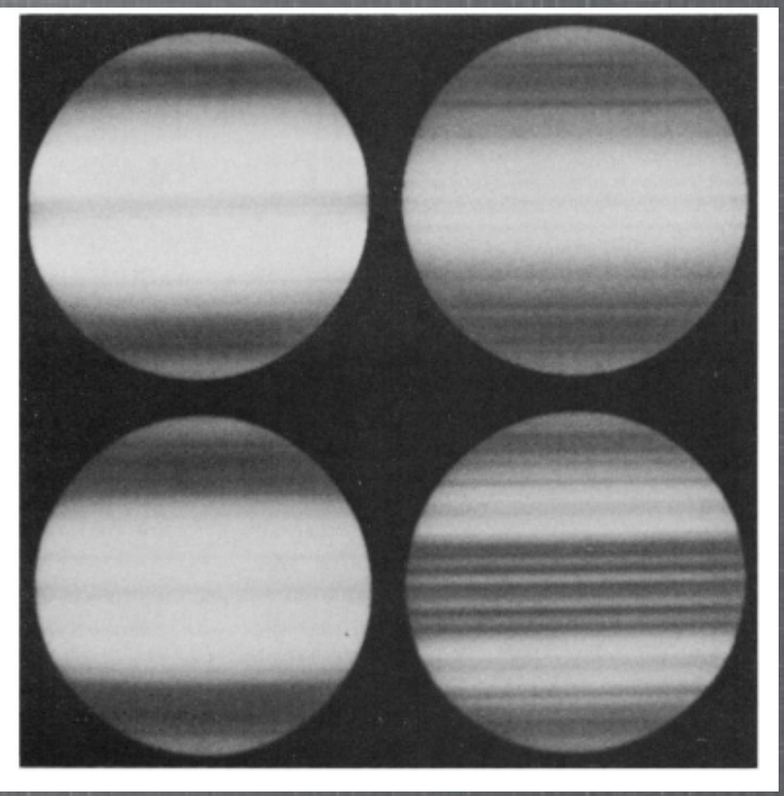

Fig. 2. The solar temperature distributions between 1983 and 1987. Sensitive measurements of the solar brightness between 1983 and 1987 at a wavelength near 500 nm and after removing faculae and sunspots would yield results corresponding to the patterns in this figure. The range from light to dark corresponds to a fractional intensity variation of about 2×10^{-3}. Starting in the upper left and moving down and then to the right column, the images correspond to the sun in the summers of 1983, 1984, 1985, and 1987.

-Changes of the solar radius: Several measurements, some are contradicting themselves (e.g. in-phase vs anti-phase variations with the SSN) ; see review by Thuillier et al. 2005.

Difficulties are due to the Earth's atmosphere, spectral domain dependence, stability of the instruments, angular calibration & data filtering techniques used.

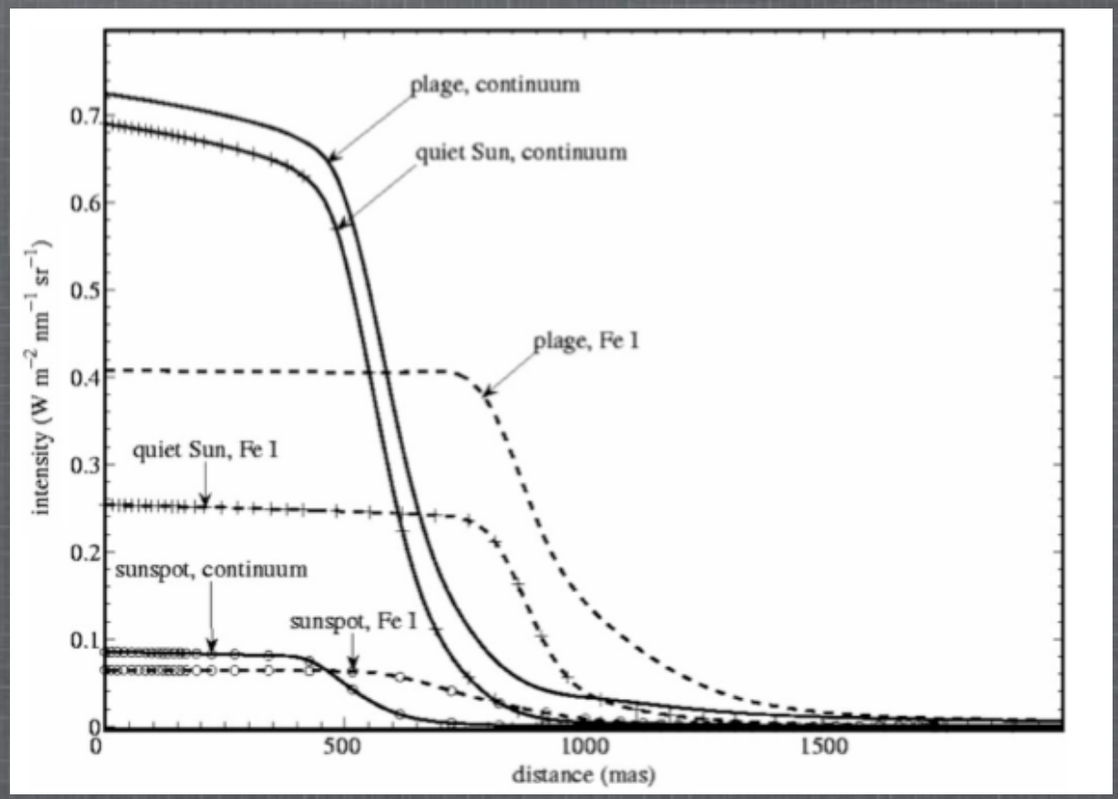

(Thuillier et al. 2005.)

Global MHD simulations of solar convection(1)

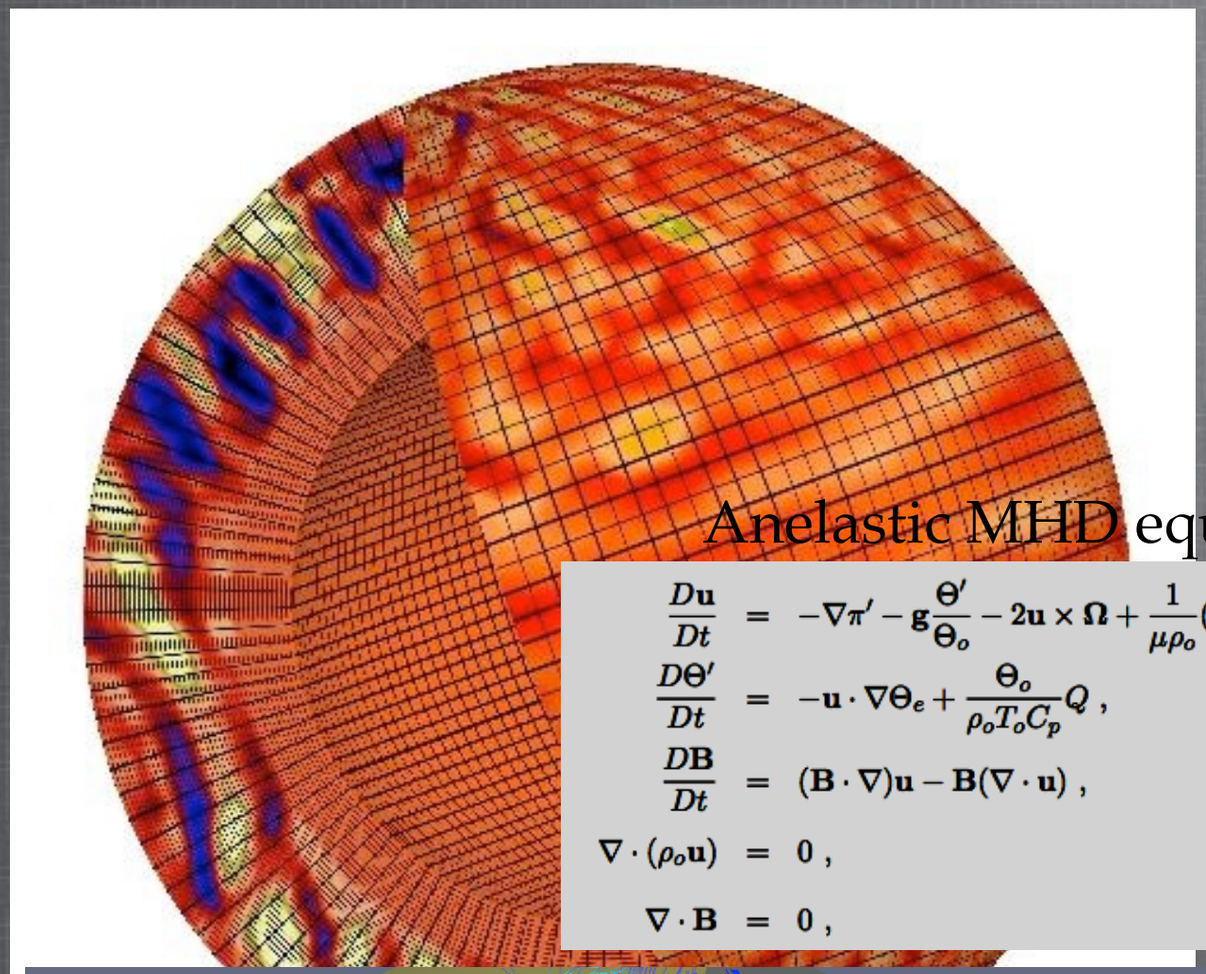

Anelastic MHD equations

$$
\begin{aligned}
\frac{D\mathbf{u}}{Dt} &= -\nabla\pi' - \mathbf{g}\frac{\Theta'}{\Theta_o} - 2\mathbf{u}\times\boldsymbol{\Omega} + \frac{1}{\mu\rho_o}(\mathbf{B}\cdot\nabla)\mathbf{B}\,, \\
\frac{D\Theta'}{Dt} &= -\mathbf{u}\cdot\nabla\Theta_e + \frac{\Theta_o}{\rho_o T_o C_p}Q\,, \\
\frac{D\mathbf{B}}{Dt} &= (\mathbf{B}\cdot\nabla)\mathbf{u} - \mathbf{B}(\nabla\cdot\mathbf{u})\,, \\
\nabla\cdot(\rho_o\mathbf{u}) &= 0\,, \\
\nabla\cdot\mathbf{B} &= 0\,,
\end{aligned}
$$

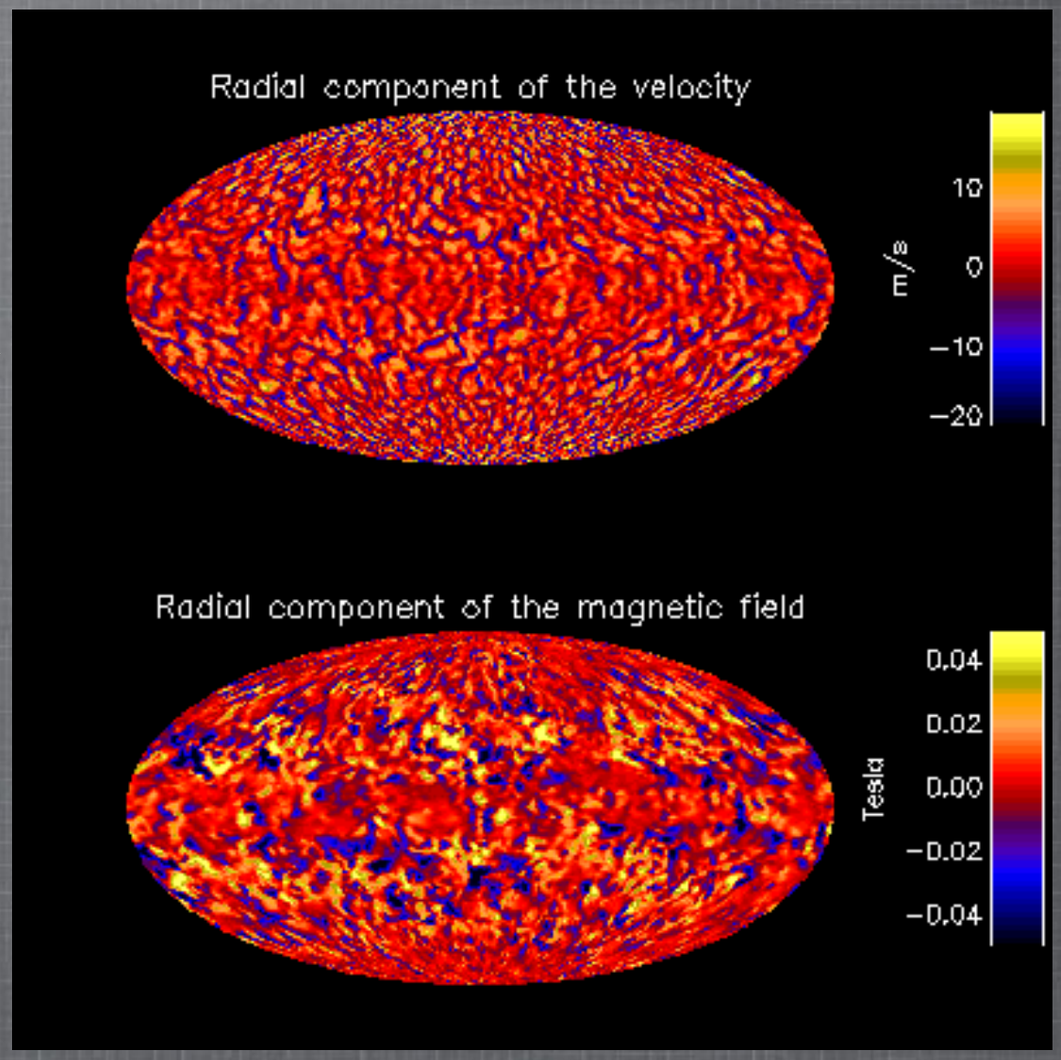

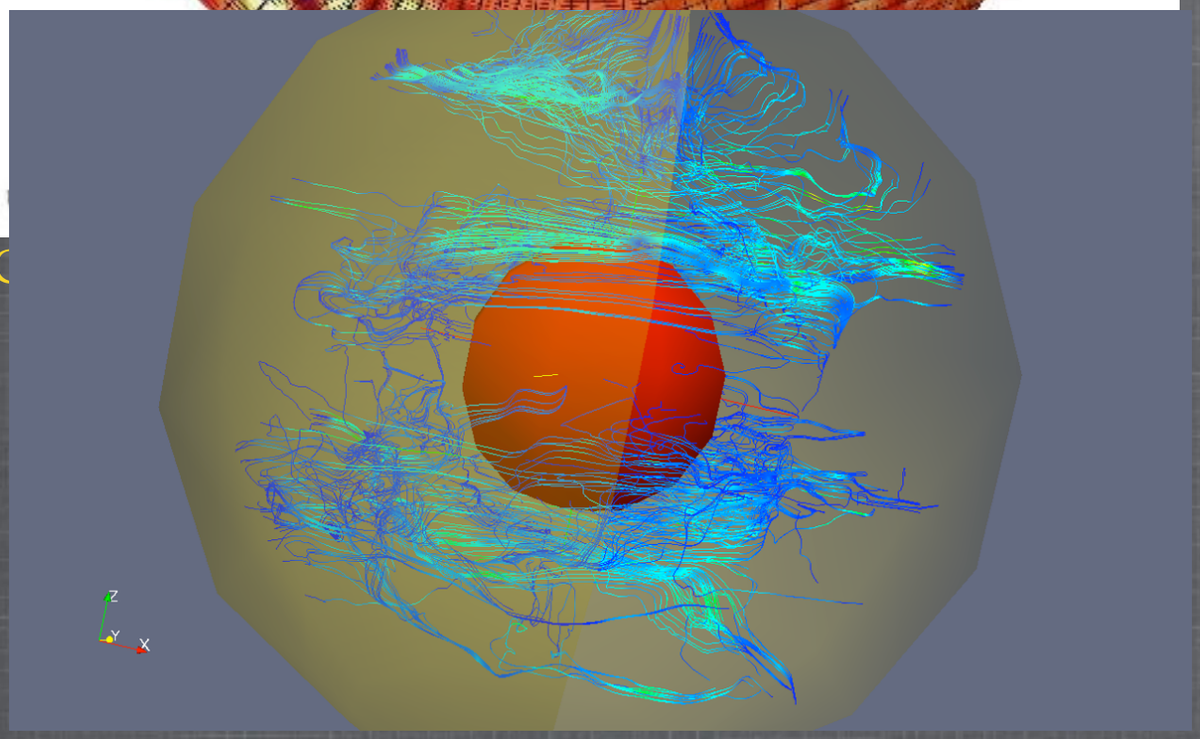

Experiments are carried out with the EULAG-MHD code (Smolarkiewicz et al. 2013). It solves the anelastic MHD equations inside a spherical shell (0.602 <r/R <0.96).

Build-up of a large-scale azimuthal magnetic field component

Global MHD simulations of solar convection(3)

The large-scale azimuthal magnetic component undergoes polarity reversals every 40 years.

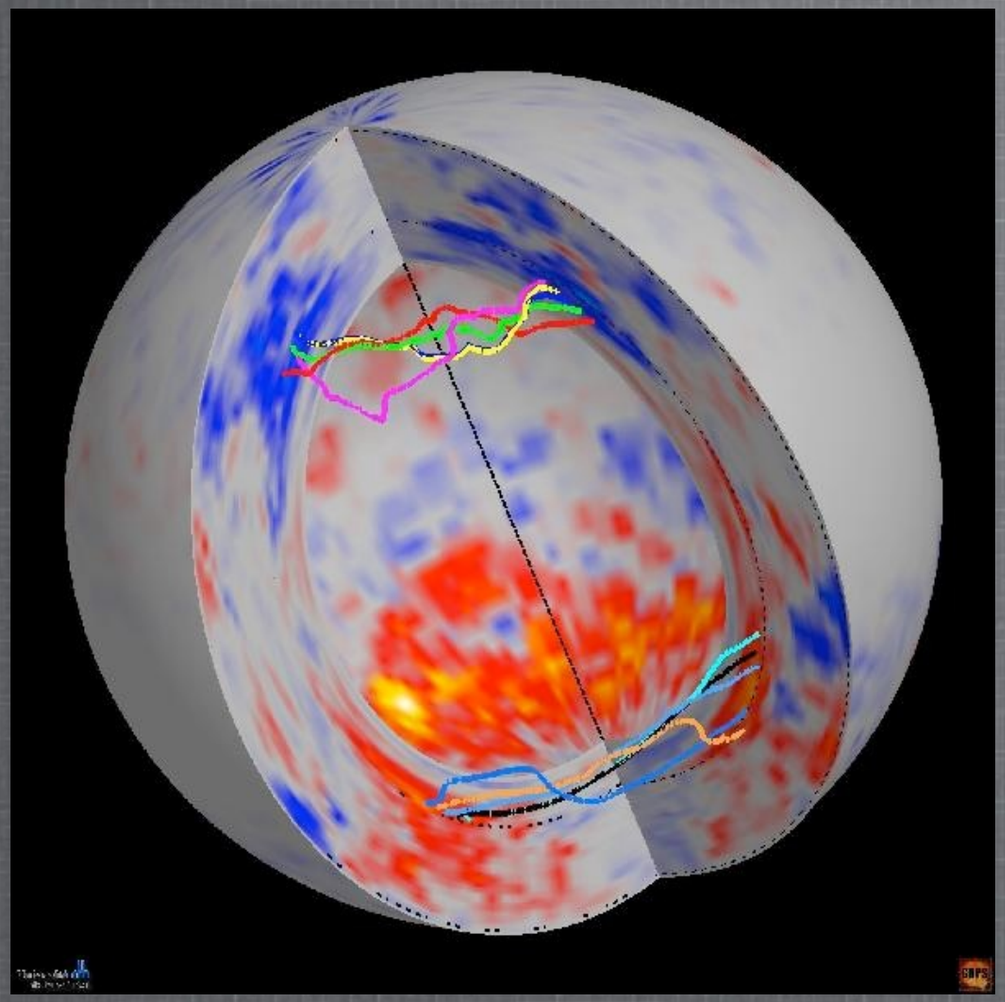

Credit: Nicolas Lawson

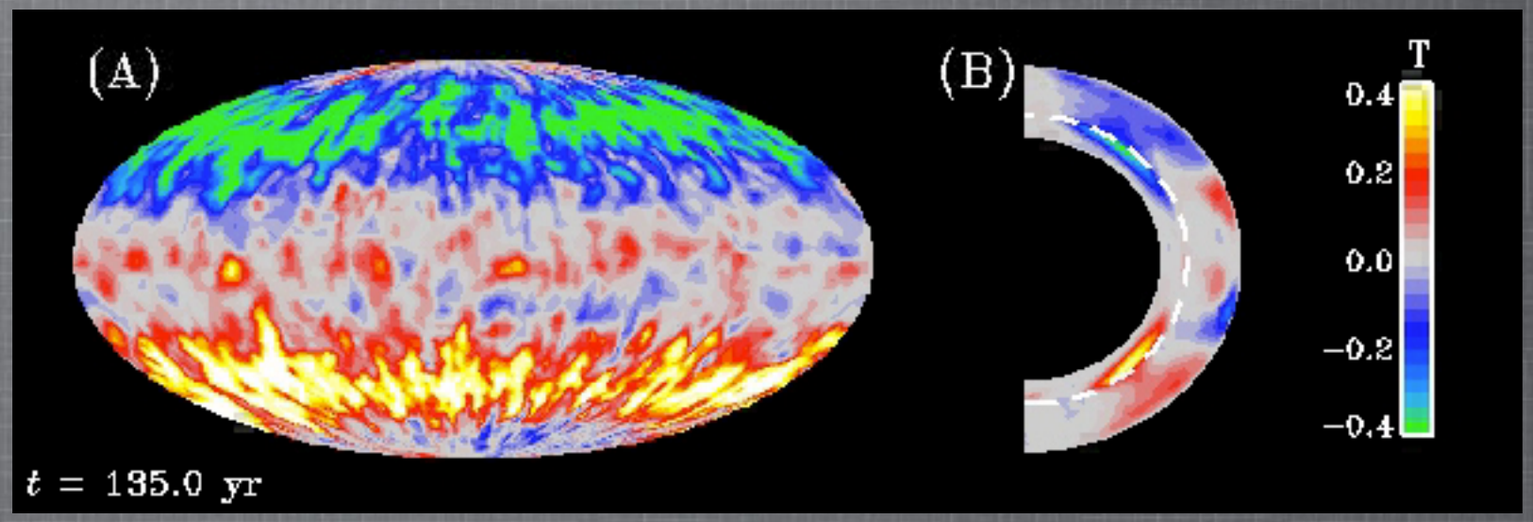

Credit: Patrice Beaudoin

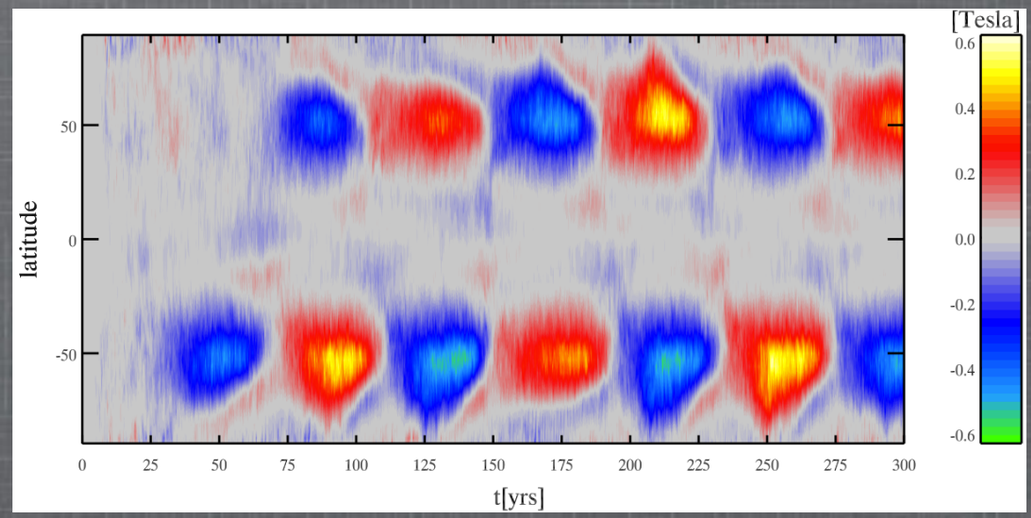

azimuthal-average of the azimuthal magnetic field component

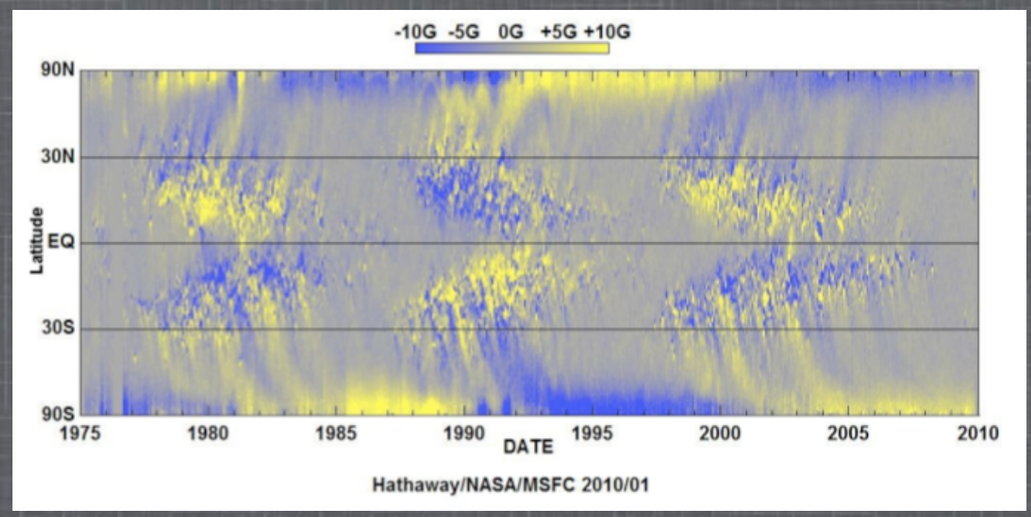

Synoptic magnetogram, Credit: David Hathaway

Global MHD simulations of solar convection(4)

The convective heat flux is the dominant player in the SCZ's energy budget.

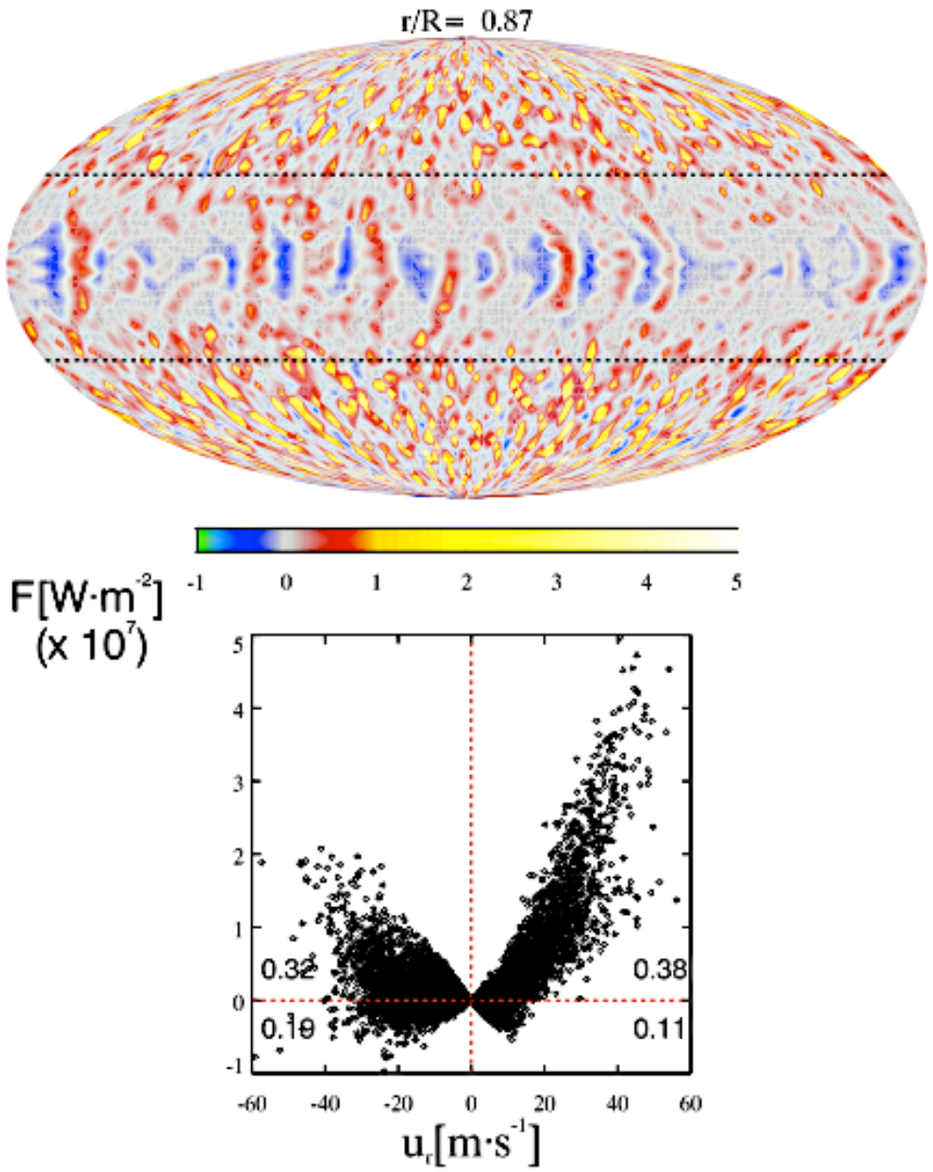

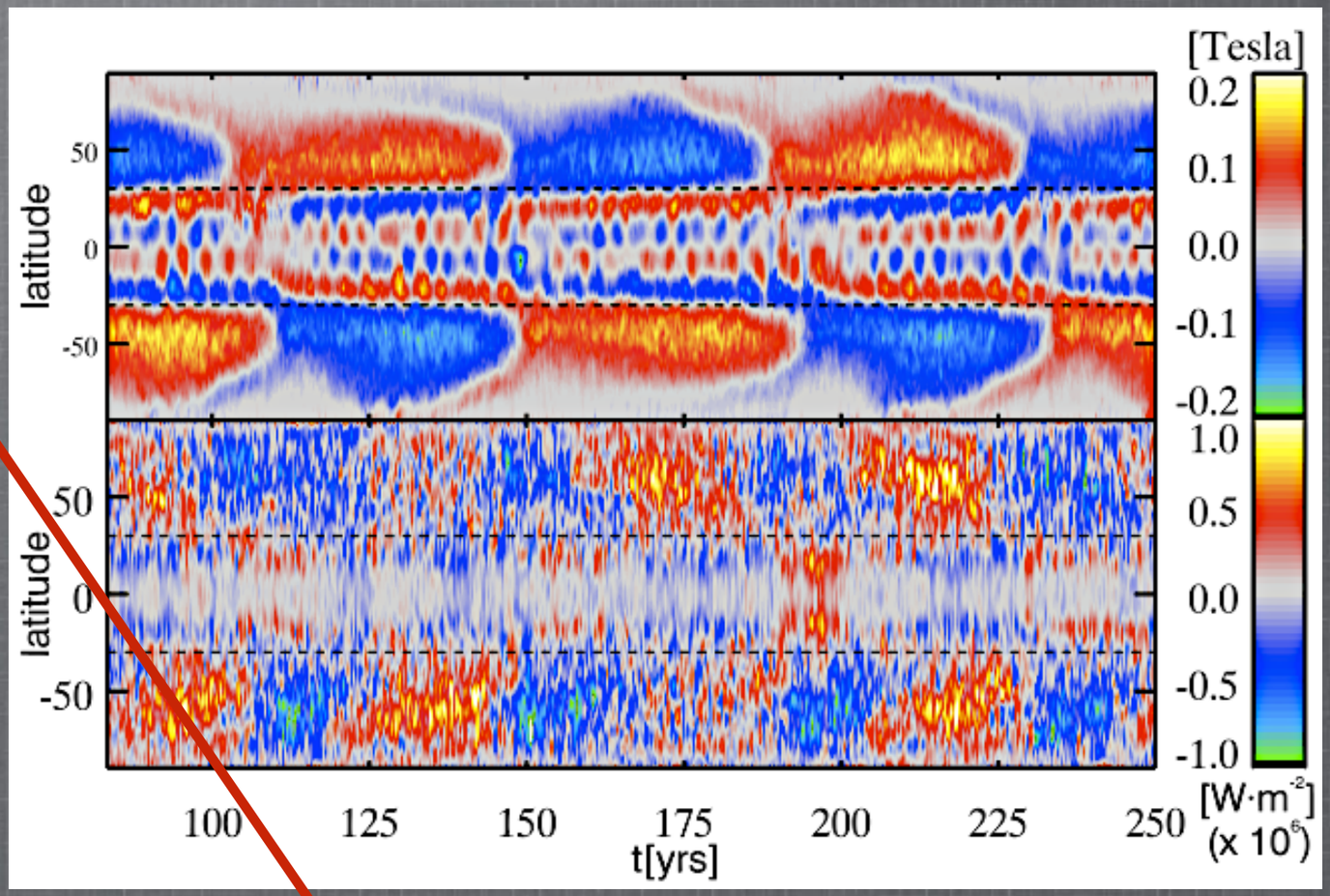

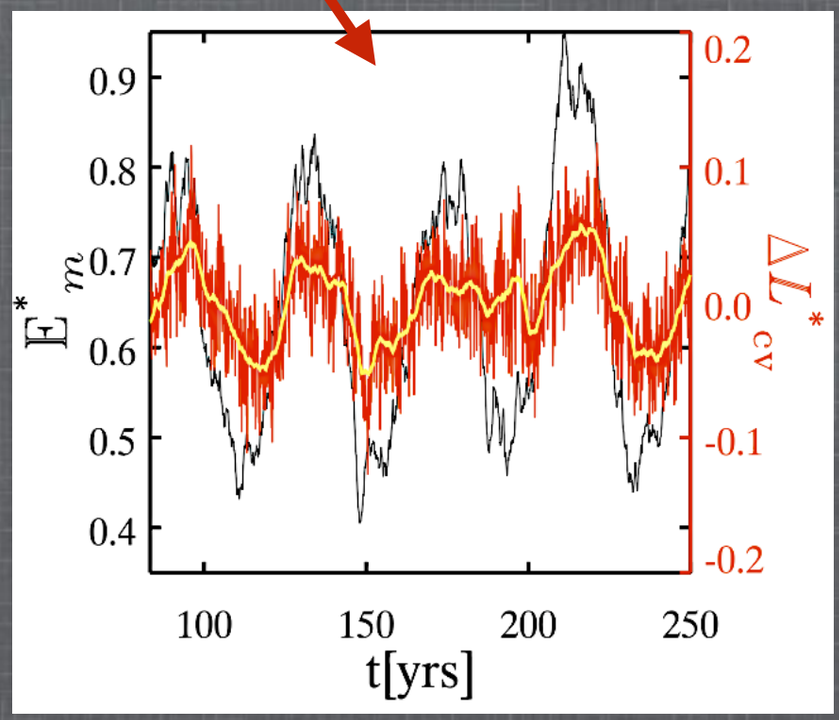

$$L_{cv} \equiv \int F \, d\sigma$$

The size of the luminosity modulation is 10% of the temporal mean luminosity.

Mean convective heat luminosity: 3% of the true solar luminosity at r=0.87R.

Cossette et al. 2013

Global MHD simulations of solar convection(5)

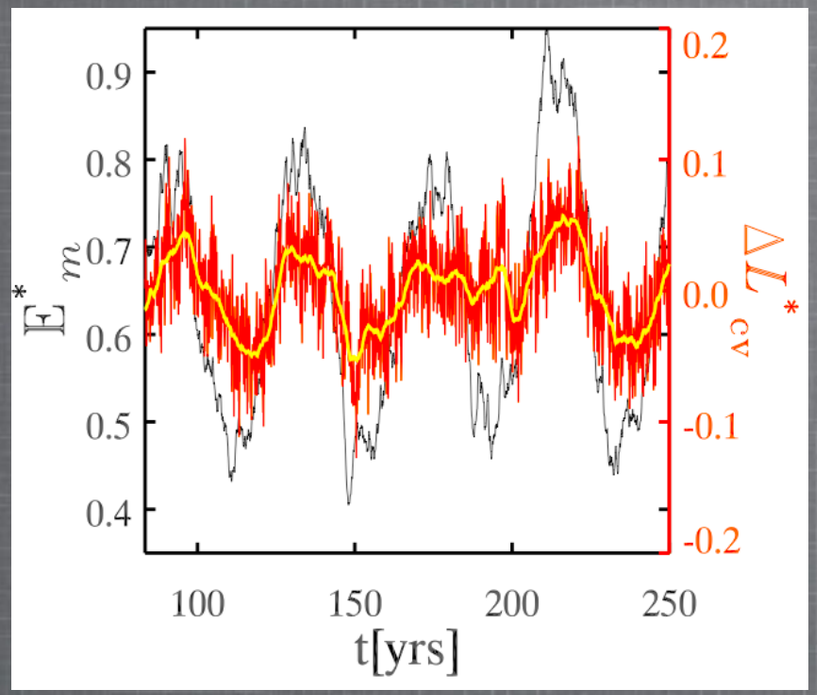

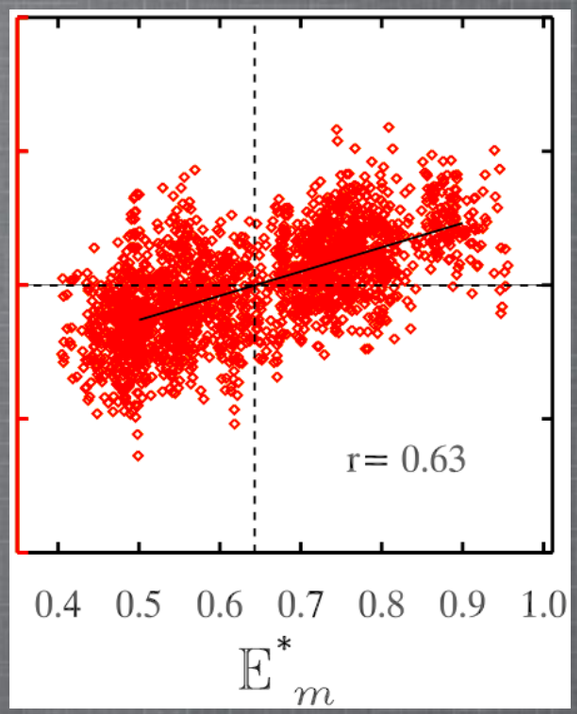

-A positive correlation between magnetic energy and convective luminosity is compatible with an enhanced value of TSI at cycle maximum.

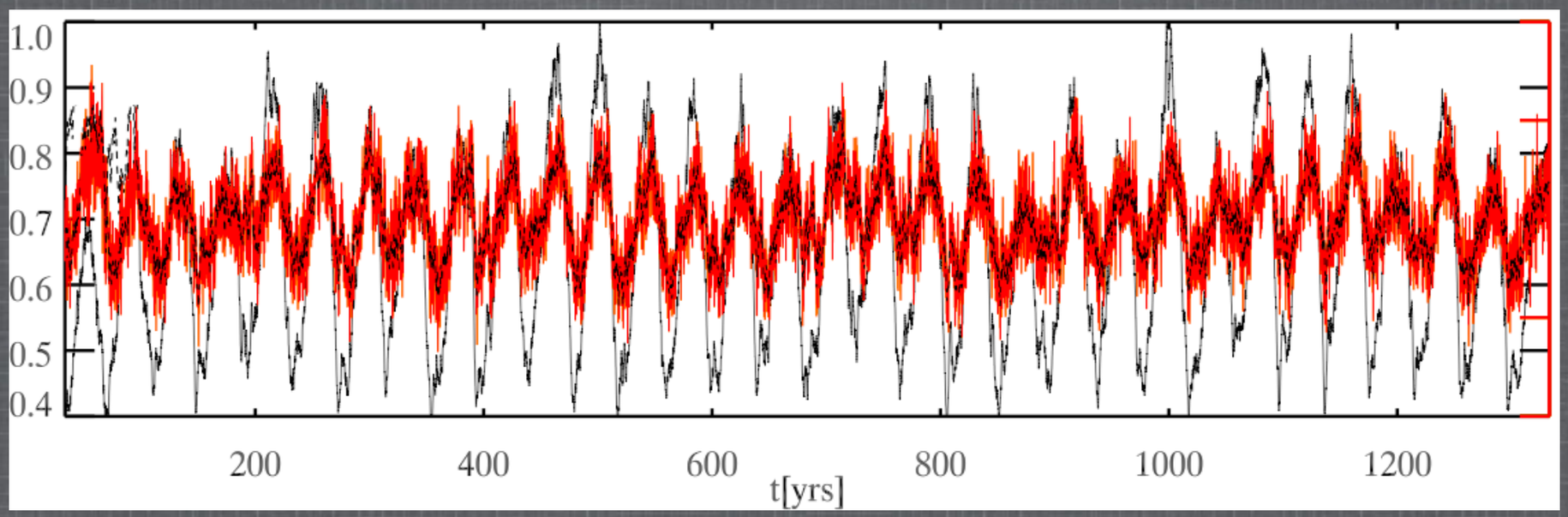

-Simulations have a low resolution (128 X 64 X 47) and can be run over very long time intervals.

Global MHD simulations of solar convection(6)

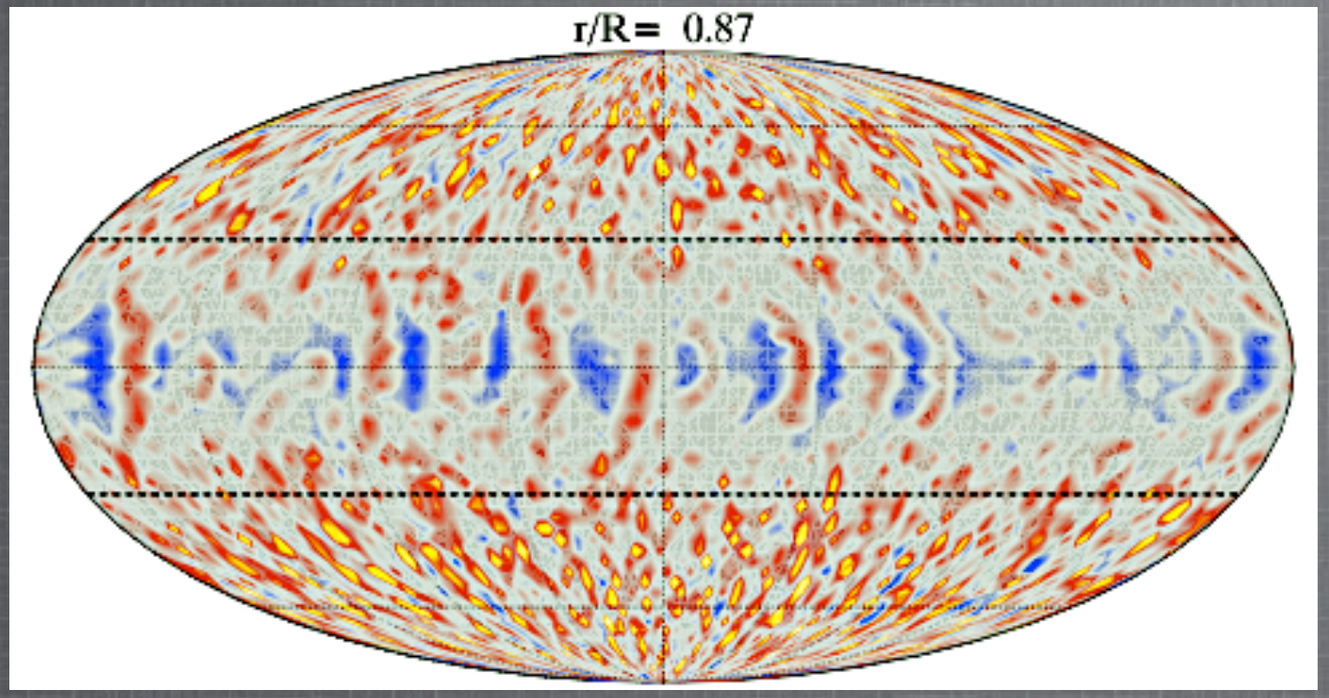

-No correlation between the vertical component of the velocity and magnetic energy implies that the modulating mechanism is more complex than the straightforward modulation of buoyancy-driven flows by the Lorentz force.

-The positive correlation between magnetic energy and thermal convective luminosity is suggestive of a magnetohydrodynamically complex process at work inside the flow.

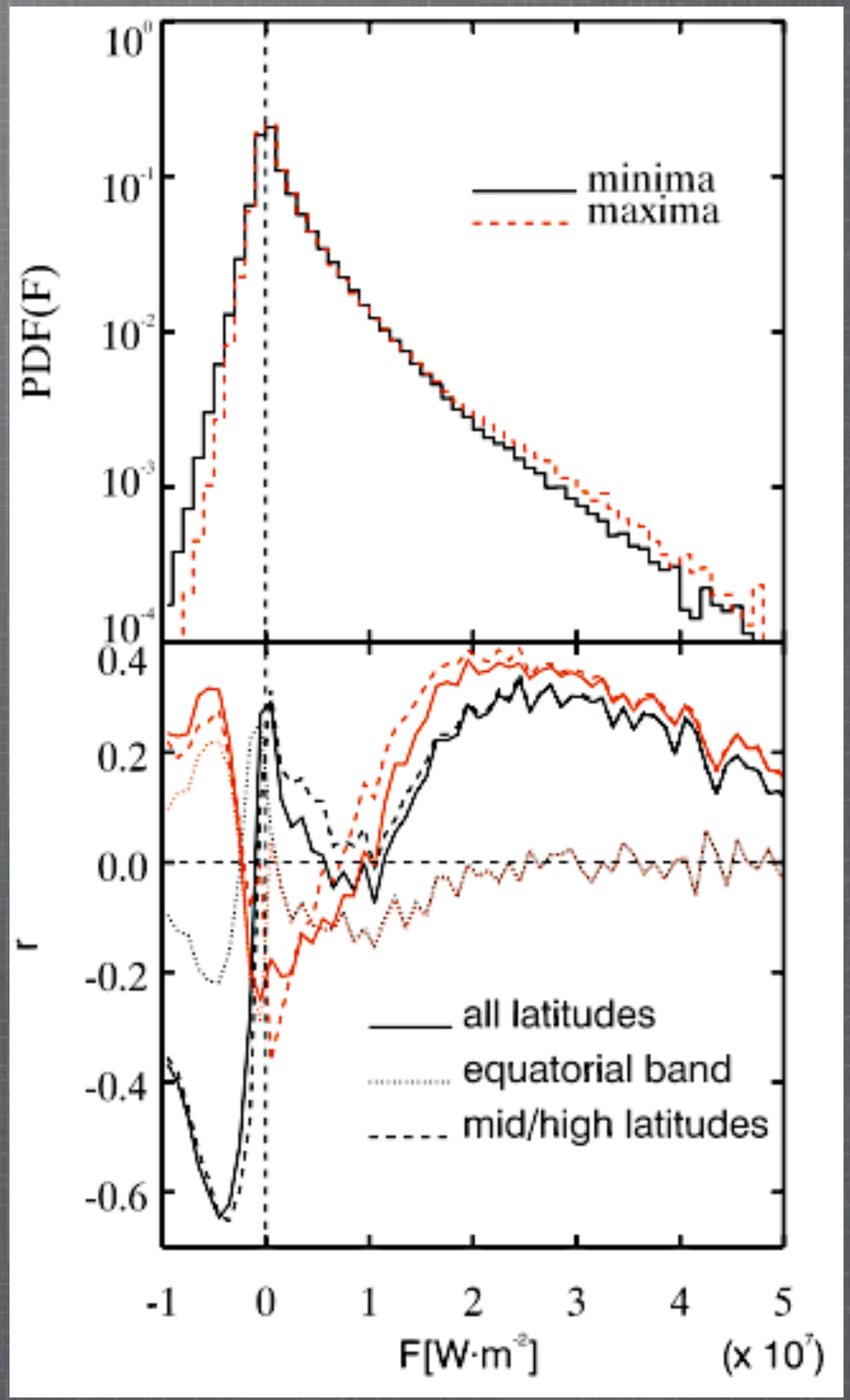

Inferring observational evidence for structural changes from MHD simulations

The observational detection of global structural changes and their influence on long-term TSI variations are extremely difficult.

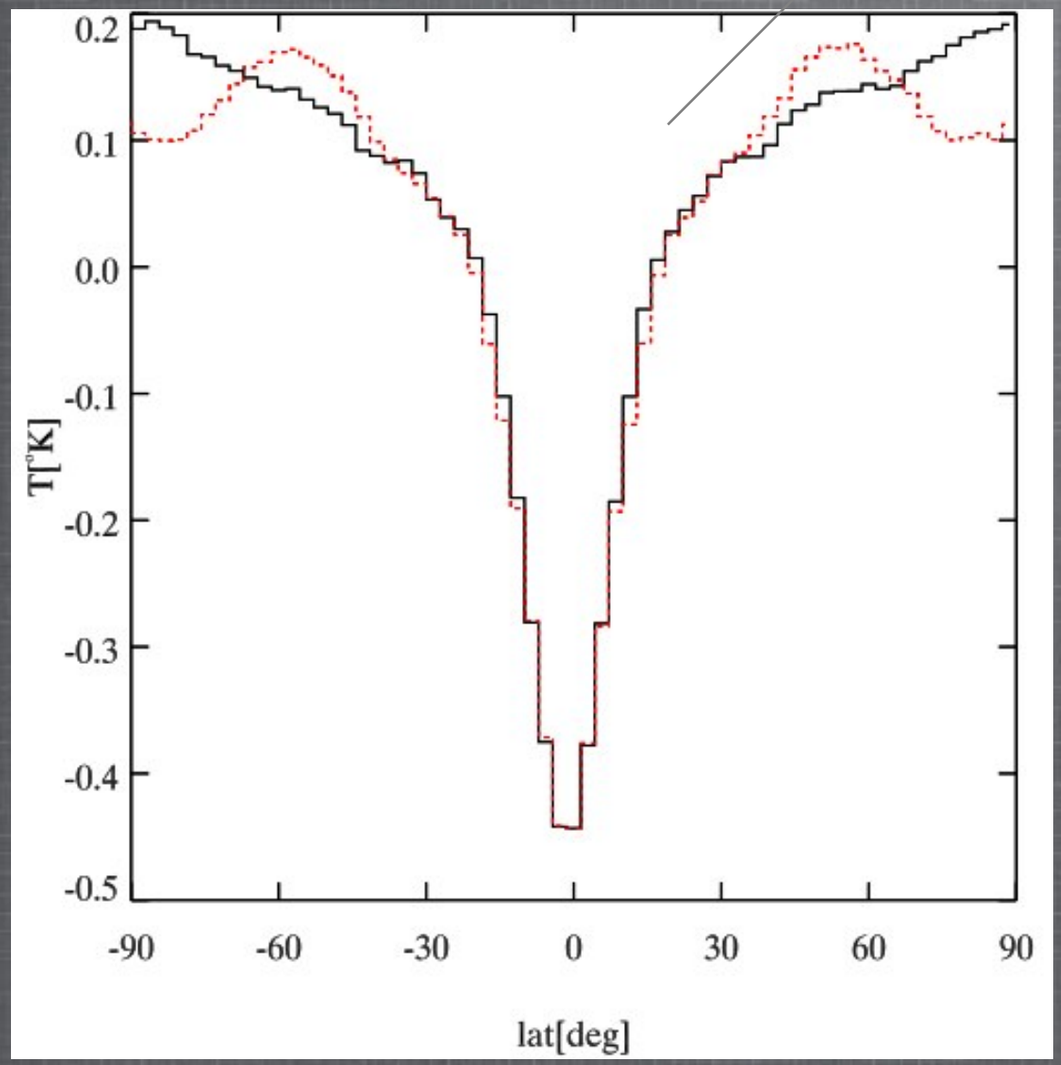

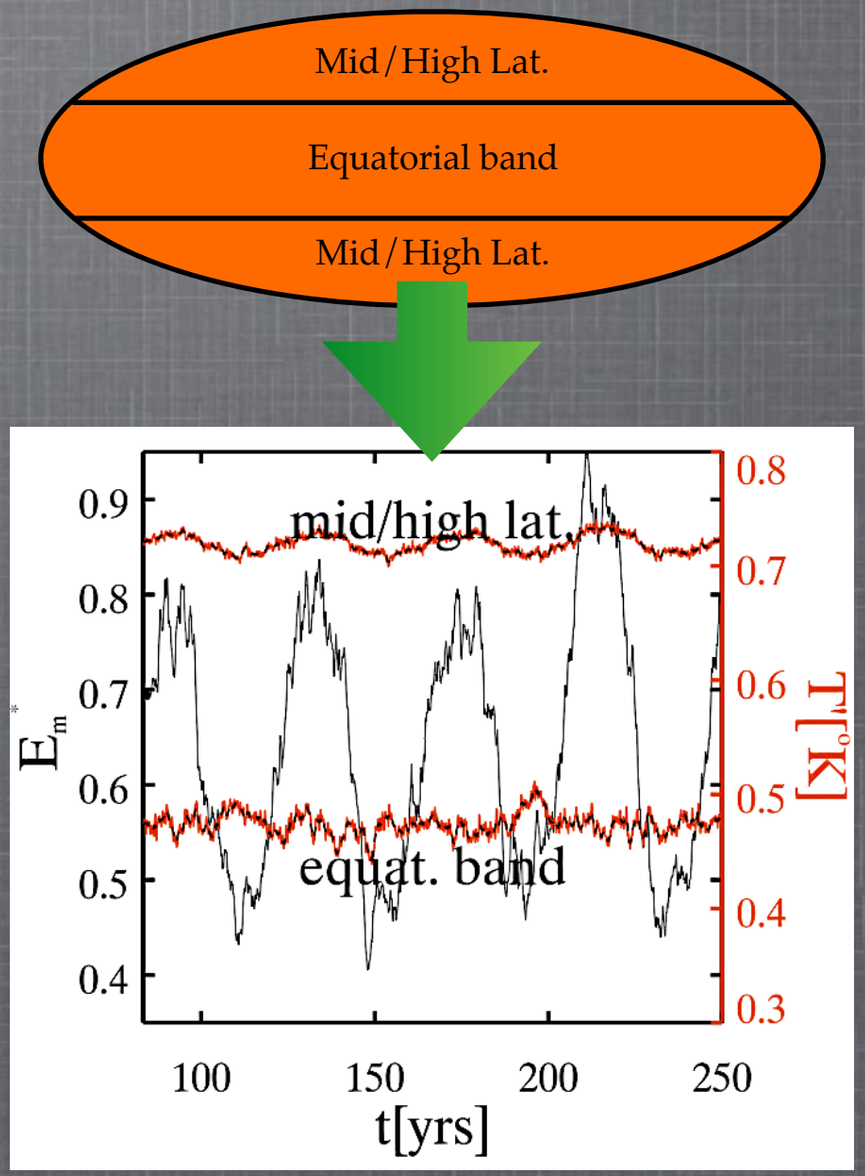

Rast et al. 2008 found a polar brightening with thermal origin.

→ Use global MHD simulations as a tool for predicting potential observational features of such changes on the Sun!

Summary & Conclusions

- Global MHD simulations now produce solar-like magnetic cycles undergoing polarity reversals on a decadal time-scale.

- The thermal convective luminosity correlates positively with magnetic energy, which is compatible with the increase of TSI that is observed at solar maximum.

- This means we now have the opportunity to predict observational signatures of potential global structural changes on the Sun by means of global MHD simulations of solar convection.

- Our current MHD model stops below the photosphere. Therefore obtaining a quantitative estimate of the amplitude of the corresponding TSI contribution will require further modelling of the upper SCZ's physical connection to the photosphere as well as carrying out a similar analysis at higher luminosity.

- We are currently performing a more detailed analysis of the modulating mechanism

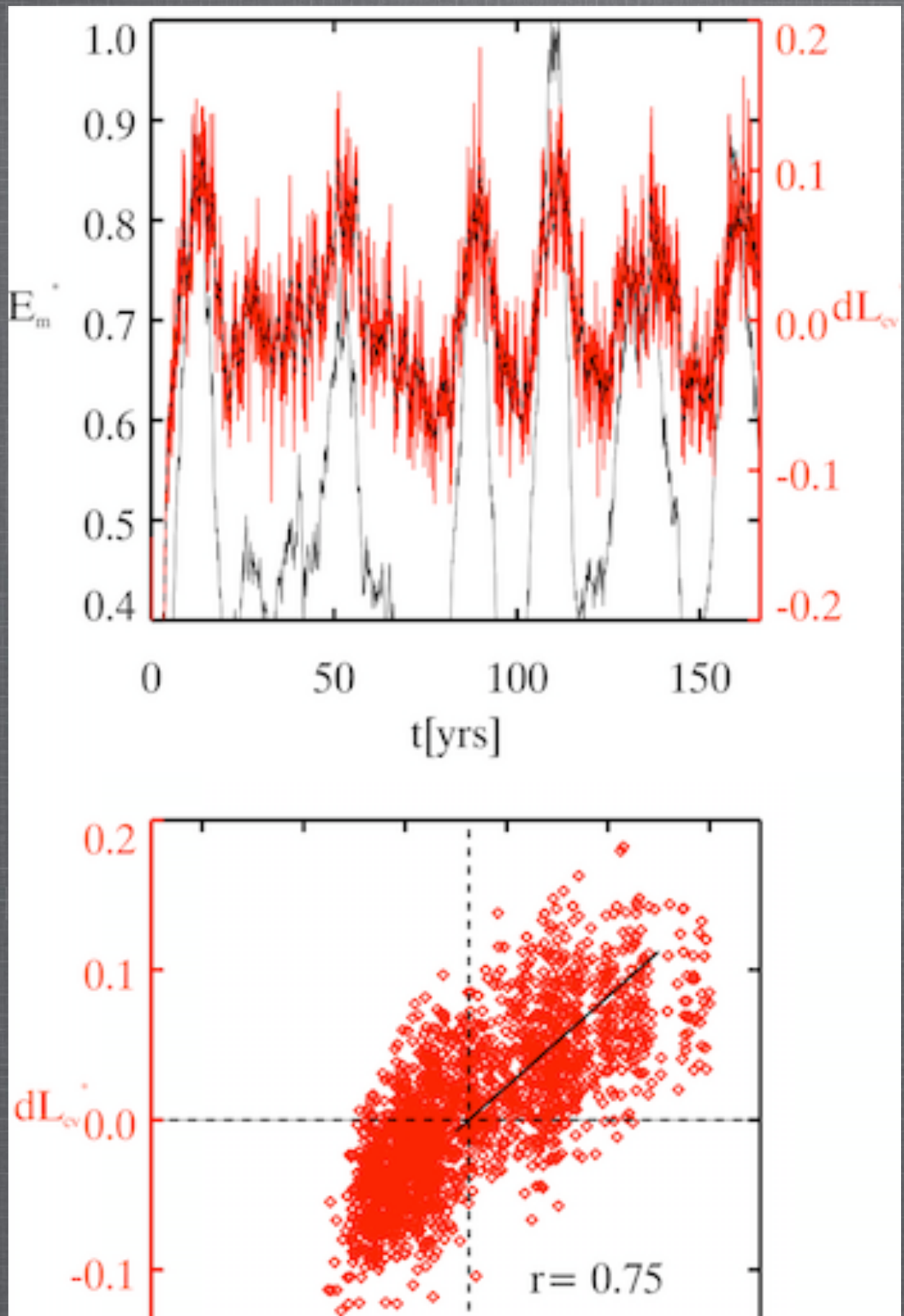
1.0
0.9
0.8
0.7
0.6
0.5
0.4
E_m
0.2
0.1
0.0
-0.1
-0.2
dL_{cv}
0
50
100
150
t[yrs]
0.2
0.1
0.0
-0.1
dL_{cv}
r= 0.75

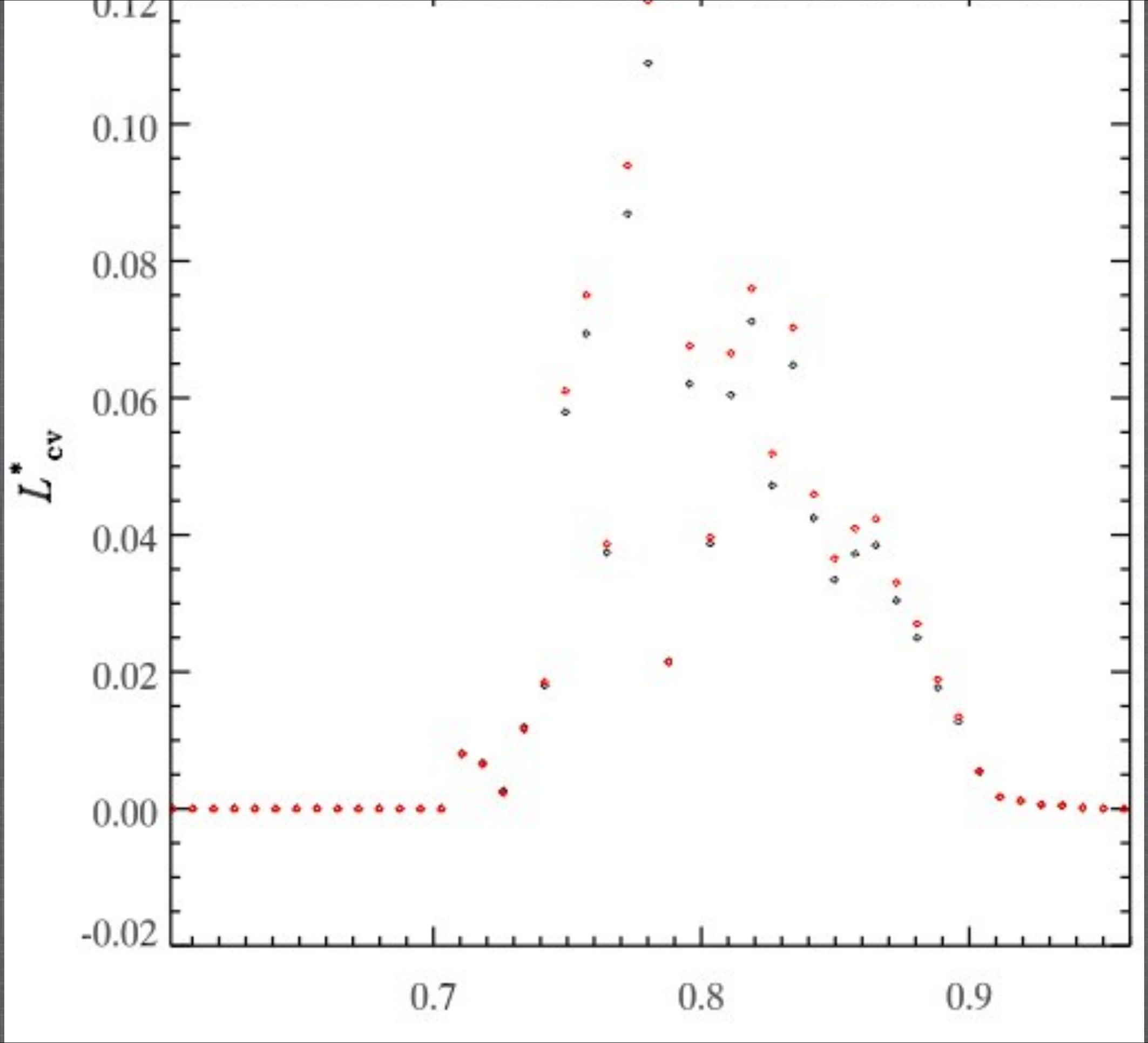
0.12
0.10
0.08
0.06
0.04
0.02
0.00
-0.02
L^*_{cv}
0.7
0.8
0.9